Wind and Rain Losses for Metal-clad Contemporary Houses Subjected to Non-cyclonic Windstorms

Hao Qin[*], Mark G. Stewart

Centre for Infrastructure Performance and Reliability
The University of Newcastle, New South Wales, 2308, Australia

17 October 2019

Abstract

Severe windstorms cause millions in losses annually for housing in Southeast Australia that has more than half of Australia's population. The risk assessment for housing in these non-cyclonic regions is the key to assessing the cost-effectiveness of relevant wind mitigation measures to reduce the economic losses. This study develops a probabilistic risk assessment framework to evaluate the wind and rain losses for Australian contemporary houses subjected to non-cyclonic windstorms, which integrates the hazard modelling for extreme wind and associated rainfall, reliability-based wind damage assessment, rainwater intrusion evaluation and economic loss modelling. The risk analysis was conducted for metal-clad contemporary houses in Brisbane and Melbourne. It was found that damage to building interior and contents caused by rainwater intrusion associated with extreme winds is the major contributor to the annual expected economic losses, and houses in Brisbane are generally subjected to higher losses than houses in Melbourne.

Keywords: Houses; Non-cyclonic windstorms; Wind and rainfall hazard; Economic losses; Probabilistic risk assessment; Rainwater intrusion.

[*]Corresponding author

1. Introduction

Non-cyclonic windstorms (e.g. synoptic storms associated with low-pressure systems; severe thunderstorms) are the major causes of wind and rainfall damage to housing in Southeast Australia. The three states, Victoria, Queensland and New South Wales, in the southeastern region have more than half of the population of Australia. Loss estimation and risk assessment for housing in these non-cyclonic regions are evidently essential and the key to assessing the cost-effectiveness of relevant wind mitigation measures to reduce the economic losses.

Losses and risks to housing during severe windstorms often accrue to damage to the building envelope (Henderson & Ginger 2008; Stewart et al. 2018). The breaches of roof cladding and windows/doors may subsequently induce significant losses to building interior and contents due to rainwater intrusion (e.g. Leitch et al. 2009; Ginger et al. 2010). Qin & Stewart (2019) recently developed a reliability-based fragility method to assess wind-induced roof damage for a representative metal-clad contemporary house in Brisbane and Melbourne. Rainfall often concurs with extreme winds. Subsequent interior and contents losses due to rainwater intrusion through the breaches of building envelope (roof and windows) can now be evaluated based on the wind fragility assessment by Qin & Stewart (2019), where a rainwater intrusion model is proposed herein.

The semi-empirical wind-driven-rain (WDR) models (e.g. Straube & Burnett 2000; Blocken & Carmeliet 2004; ISO 2009) have initially been developed for the assessment of moisture, hygrothermal and durability of building facades. The development of the semi-empirical relationships is based on experimental and/or field observations that the amount of WDR depositing on buildings increases approximately proportionally with wind speed and rainfall intensity (Blocken & Carmeliet 2004). Numerical modelling using computational fluid dynamics (CFD) provides an alternative approach for more detailed quantification of WDR (e.g. Choi 1994a; Blocken & Carmeliet 2002). Recently, these WDR methods have been

extended to evaluate the amount of rainwater intrusion through building envelope breaches during hurricanes for timber-framed houses in the US (Dao 2010; Dao & van de Lindt 2010; Pita et al. 2012; Baheru et al. 2015; Johnson et al. 2018; Pant & Cha 2019). Although the CFD approach provides a more detailed assessment of WDR, it increases the complexity and cost in both modelling and computation (Blocken & Carmeliet 2010). This may not be suitable for roofs of Australian contemporary houses with large dimensions and complex geometries. The semi-empirical WDR model is thus employed in this study for a convenient and fast evaluation of rainwater intrusion. In this study, the semi-empirical WDR model is modified to suit metal-clad contemporary houses in Australia subjected to non-cyclonic winds. Rainwater intrusion through damaged windows and gaps around undamaged windows that are commonly reported in post-damage investigations (Henderson & Ginger 2008; Ginger et al. 2010; Henderson et al. 2017) is also considered in this study.

The loss estimation and risk assessment for houses in the US are based on existing wind and rainfall models for hurricanes (e.g. Pita et al. 2012; Johnson et al. 2018; Pant & Cha 2019). However, there is a lack of hazard models for rainfall associated with non-cyclonic extreme winds. Thus, this study newly develops a probabilistic model to characterize the duration and the average rainfall intensity for non-cyclonic windstorms using regional wind and rainfall data of Brisbane and Melbourne. This model can be used for the subsequent rainwater intrusion assessment after wind damage. Loss estimation is conducted based on cost data obtained from Australian housing cost guides (Rawlinsons 2015). The loss functions is dependent on the extent of wind damage to housing components and the volume of rainwater intrusion yielded by the wind fragility analysis and the rainwater intrusion model, respectively, and are developed according to the loss modelling in HAZUS (2014) and engineering judgement. By integrating the hazard model for extreme wind and associated rainfall, wind damage and rainwater intrusion assessment, and loss modelling, this study conducts a probabilistic risk

assessment for the representative contemporary house in Brisbane and Melbourne. The obtained annual expected economic losses can further facilitate the risk mitigation and climate adaptation for housing in non-cyclonic regions of Australia.

2. Risk Assessment Framework

The risk from extreme winds is expressed as (Stewart et al. 2018)

$$E(L) = \sum \Pr(H) \Pr(DS|H) \Pr(L|DS) L \tag{1}$$

where $\Pr(H)$ is the probability of a wind hazard. The wind hazard is typically represented by the wind speed, which can be further extended to include other environmental hazard of interest (e.g. rainfall, windborne debris, storm surge) commonly associated with or induced by the extreme wind event. $\Pr(DS|H)$ is the probability of a damage state conditional on the hazard (fragility), $\Pr(L|DS)$ is the conditional probability of a loss given occurrence of the damage, and L is the loss or consequence if full damage occurs. According to post-damage surveys (e.g. Leitch et al. 2009), the majority of losses to contemporary houses result from wind damage to roof and fenestrations (especially windows), and the subsequent rainwater damage to building interior and contents. Wind-induced damage to other housing components (e.g. walls) is rare for contemporary houses in non-cyclonic regions of Australia. Therefore, the possible losses considered in this study arise from wind damage to metal roof cladding and timber roof framing, windward windows, and rainwater damage to building interior and contents as well as the loss of use.

3. Hazard Modelling

3.1. Extreme wind speed

The peak gust wind speed in non-cyclonic regions of Australia, v (m/s), is modelled by a Gumbel distribution. The cumulative distribution function (CDF) for annual maximum gust wind speed is given by (Wang et al. 2013; Stewart et al. 2018)

$$F_V(v) = e^{-e^{-\frac{v - v_g}{\sigma_g}}} \tag{2}$$

where v_g and σ_g are the location and scale parameter, respectively. The gust wind speed v is the maximum 0.2 second gust velocity at 10 m height in open terrain. Figure 1 depicts the extreme gust wind speed corresponding to various return periods. The location and scale parameters are given as v_g=26.0326, σ_g=4.0488 for Brisbane and v_g=27.7777, σ_g=1.664 for Melbourne (Wang et al. 2013; Stewart et al. 2018).

3.2. Rainfall associated with extreme winds

An extreme wind event is often associated with rainfall. When assessing rainwater intrusion and the consequent damage to building interior and contents, it is ideal to have the joint probability of wind speed and rainfall intensity rather than treating these two weather variables independently. In addition, the average rainfall intensity (R_h) during a windstorm is typically dependent on the duration, e.g. intense burst of rainfall is more likely to occur in a short event.

The exponential distribution is connected to the Poisson arrival process, and commonly used to model the storm duration (e.g. Eagleson 1972; Koutsoyiannis & Georgiou 1993; Lambert & Kuczera 1998). A two-parameter exponential distribution is adopted in this study to model the windstorm duration (D_{ur}) with the CDF given by

$$F(D_{ur}) = 1 - e^{-\lambda(D_{ur} - \mu)} \tag{3}$$

where λ and μ are the rate and location parameter, respectively.

A gamma distribution is used to model the average rainfall intensity during an extreme windstorm. The probability density function (PDF) of the gamma distribution is given by

$$g(R_h) = \frac{R_h^{\gamma - 1} e^{\frac{R_h}{\beta(D_{ur})}}}{\Gamma[\gamma] \beta(D_{ur})^\gamma} \tag{4}$$

where $\Gamma(\cdot)$ is the gamma function, γ is the shape parameter, and $\beta(D_{ur}) = a_0 + a_1(1/D_{ur})$ is the scale parameter which is assumed to have a linear relationship with the reciprocal of D_{ur}. Note

that R_h in Eq. (4) is greater than zero, and hence the gamma distribution is only used when rainfall occurs simultaneously with strong winds. Accounting for the probability of no rain (P_{no}) during a windstorm, the CDF of R_h ($R_h \geq 0$) is given by

$$F(R_h) = P_{no} + (1 - P_{no})G(R_h) \qquad (5)$$

where $G(R_h)$ is the CDF of the gamma distribution given by Eq. (4) to model the non-zero R_h, and P_{no} can be estimated from the meteorological data.

The model parameters of the exponential and gamma distribution are estimated using the meteorological data from two weather stations, i.e. Archerfield airport in Brisbane and Moorabbin airport in Melbourne. A twenty-year length of half hourly wind and rainfall data from 1996 to 2015 for these two weather stations are obtained from the Australian Bureau of Meteorology (BoM). A windstorm with the maximum gust wind speed greater than 36 knots (i.e. 18.5 m/s or 66.7 km/hr) is considered as an extreme wind as strong wind warnings can be issued at this wind speed by BoM. A total of 86 and 364 severe windstorms from 1996 to 2015 are then extracted from the meteorological data for Archerfield and Moorabbin airports, respectively, and for each storm event, the duration and average rainfall intensity (accumulative rainfall depth divided by storm duration) are obtained. The number of storm events with no rain (i.e. $R_h = 0$) is also obtained to estimate P_{no}.

Figure 2 shows the exponential probability plots for D_{ur}, which suggests that the two-parameter exponential distribution given by Eq. (3) fits well to the storm duration data. It is estimated that $P_{no} = 25.6\%$ and 45.9% for Brisbane and Melbourne, respectively. The model parameters in the gamma regression formulation given by Eq. (4) are estimated using the generalized linear model in the R software package (R Core Team 2019). Figure 3 shows the mean and quantile values produced by the gamma model as a function of D_{ur}. The average rainfall intensity data is also plotted in the same figure, which indicates that Brisbane tends to have shorter windstorms with more intense rainfall (e.g. thunderstorms), whereas windstorms

in Melbourne are generally longer with lower average rainfall intensity. Figure 3 suggests a good predictability of the gamma model to capture the average rainfall intensity during windstorms. Note that the estimated model parameters for D_{ur} and R_h can only be rigorously applied to the risk assessment for houses in the surrounding or nearby suburbs of Archerfield airport and Moorabbin airport, however it can be further extended to incorporate more weather stations in Brisbane and Melbourne, and account for the spatial variations and patterns of rainfall. Other probability distributions, e.g. Weibull, lognormal, Generalized Pareto, have also been reported in the literature to model the rainfall intensity (e.g. Heneker et al. 2001; Koutsoyiannis et al. 2003; Mudd et al. 2016), however, it is out of the scope of this study to examine which is the best fit to the local meteorological data. The accuracy of estimation can be further improved by incorporating more years of data, if available.

4. Wind Damage

4.1. Roof fragility

A reliability-based fragility method has been developed by Qin & Stewart (2019) to assess the wind damage to metal roof cladding and timber roof trusses for Australian contemporary houses. The fragility analysis was conducted for a representative contemporary house in the Australian suburbs of Brisbane and Melbourne. The house has a complex hip roof and is a wood-frame brick-veneer construction with a roof slope of 21.5°. Windows are generally sliding or awning windows with a brick on edge or terracotta tiled window sill. Corrugated metal roof sheets are installed and connected to metal top-hat battens. Figure 4 depicts the 3D and plan view of the representative one-storey house. See Parackal et al. (2016) for more details.

The fragility of the roof system is defined as the extent of roof sheeting loss and roof truss failures at a given gust wind speed. The overloading of cladding-to-batten (CTB), batten-to-rafter/truss (BTR) and rafter/truss-to-wall (RTW) connections is considered to cause the failure

of metal roof sheeting and timber roof trusses as these roof connections are generally the 'weakest links' of the roof system (Henderson & Ginger 2007). The limit state function for a single roof connection is

$$g = R - (W - D_L) \qquad (6)$$

where R is the connection resistance, W is the wind uplift loads acting on this connection, and D_L is the dead load accounting for the weight of roof components. A connection is deemed to fail if $g \leq 0$. The probabilistic models for the wind loading and connection resistances are given by Qin & Stewart (2019). The uplift forces in roof connections are obtained using a FE approach described in Qin & Stewart (2019).

In the fragility analysis, two typical scenarios are assumed for the internal pressurization, i.e. (i) the existence of windward dominant openings, and (ii) without any wall openings. A Monte Carlo Simulation (MCS) analysis in conjunction with the FE approach are employed to assess the wind fragility for roof cladding and trusses, which enables the probabilistic characterization of spatially varying wind uplift pressures, uplift forces in roof connections, progressive failure and load redistribution after initial local damage, and internal pressure changes with increasing sheeting loss. A total of 1,646 CTB, 532 BTR and 38 RTW connections are involved in the MCS analysis and FE approach. The fragility curves yielded by the MCS and FE approach express the extent of roof sheeting loss (R_{clad}) and the proportion of roof truss failures (R_{truss}) as a function of gust wind speed. According to AS4055 (2012), suburban houses in Brisbane generally have design wind classifications of N2 and N3, and those in Melbourne are typically with design wind classifications of N1 and N2. The mean proportions of roof sheeting loss and roof truss failures produced by the fragility assessment are shown in Fig. 5. The RTW connectors are different for houses with design wind classifications of N1, N2 and N3. Note that the fragility results apply to suburban houses (i.e. the nominal value for terrain and height factor is 0.83 as given by AS/NZS 1170.2 2011) on a

flat site without shielding and wind directionality effects but have the flexibility to account for other site conditions. Refer to Qin & Stewart (2019) for more details about the fragility analysis.

4.2. Window damage

The windward dominant openings and associated rainwater intrusion are considered to result from the breakage of windows by high wind pressure. The wind pressure acting on the windward window (W_{win}) is calculated based on the gust wind speed and the wind loading parameters (e.g. terrain and height factor, shielding factor, wind directionality factor, pressure coefficients, etc.). An external wall pressure coefficient is assumed to follow a normal distribution with a mean of 0.70 and a coefficient of variation (COV) of 0.15 (Henderson & Ginger 2007). The internal pressure coefficient is calculated based on the approach given by Qin & Stewart (2019) considering the failure progression of metal roof sheets. Note that window failure caused by windborne debris is not considered in this study because the damage assessment is only conducted for a single house instead of a residential community where debris are often generated from neighbourhood houses. In addition, windborne debris is less of a concern in non-cyclonic regions of Australia as indicated in AS/NZS 1170.2 (2011).

According to AS2047 (2014), windows shall not fail when tested under the ultimate limit state pressure, and shall not have penetration of uncontrolled water when tested under the water penetration resistance test pressure. The ultimate strength (R_{ult}) and water penetration resistance (R_{water}) of windows are assumed to follow a normal distribution (HAZUS 2014). It is further assumed that the COV is 0.20 and that 20% of the windows do not satisfy the test pressures specified in AS2047 (2014) to account for the variance of quality in manufacture and installation (HAZUS 2014). In other words, the mean ultimate strength and water penetration resistance are about 1.20 times the test pressures specified in AS2047 (2014). The statistics for window resistances are given in Table 1, and the limit states used for windward windows are shown in Table 2.

5. Rainwater Intrusion

The quantification of rainwater intrusion is also conducted under two wall opening scenarios: (i) with windward dominant openings (with window breakage) and (ii) without any wall openings (without window breakage). For the dominant opening scenario, the main source of rainwater intrusion considered is water entering from roof and window breaches. Due to high wind pressures acting on the windward wall during an extreme wind event, water entry through undamaged windows has been commonly reported in post-damage surveys (Henderson & Ginger 2008; Ginger et al. 2010). This is likely because the high differential pressures across windows exceed the water penetration resistances of windows. For the scenario without any wall openings, rainwater is thus considered to enter through roof breaches and gaps around windward windows. The rainwater intrusion via any gaps and cracks on undamaged roof cladding is neglected because the metal roof is mostly subjected to suction pressures, and is generally more watertight.

Given the occurrence of strong wind, the rain is endorsed a horizontal velocity by the wind and then falls obliquely. The vertical component of the oblique rainfall passing through a horizontal plane is typically measured at the meteorological stations, while the horizontal component passing through a vertical plane, defined as wind-driving rain (WDR), is not measured and needs to be quantified by relevant WDR methods. A semi-empirical WDR model (e.g. Straube & Burnett 2000; Blocken & Carmeliet 2004; ISO 2009) is employed in this study to assess the amount of driving rain entering the breaches and gaps in the building envelope. An empirical runoff model is also applied to assess the water ingress due to rainwater runoff from upstream undamaged building envelope.

5.1. Free-field WDR intensity

It is assumed that the wind flow is uniform, steady and horizontal, and the horizontal velocity of the raindrops is equal to the wind speed. Then the free-field WDR intensity

(unobstructed by the building), R_{WDR} (mm/hour), passing through an imaginary vertical plane is given by (Straube & Burnett 2000; Blocken & Carmeliet 2004)

$$R_{WDR} = DRF \cdot R_h \cdot U \qquad (7)$$

where U (m/s) is the mean wind speed, R_h (mm/hr) is the average rainfall intensity, $DRF = 1/V_t$ is the driving rain factor, and V_t (m/s) is the terminal velocity of raindrops (i.e. vertical falling speed of raindrops). The driving rain factor DRF is a function of the rainfall intensity R_h, and is evaluated using the approach given by Choi (1994b). Table 3 shows the DRF values corresponding to various rainfall intensities.

The mean wind speed, U, can be linked to the maximum gust wind speed, v, by the following equation

$$U = (E \cdot D \cdot T) \cdot v/G_u \qquad (8)$$

where E is the terrain height factor to model the exposure and building height, D is a factor for wind directionality effects, T is the shielding factor, and G_u is the velocity gust factor used to approximately convert a peak gust wind speed to corresponding mean wind speed. The factors E, D and T are assumed to follow a lognormal distribution with the mean-to-nominal ratios and COV values given in Qin & Stewart (2019). The corresponding nominal values of these factors can be obtained from AS/NZS 1170.2 (2011) for different site conditions. For an hourly mean wind speed, a gust duration of 0.2s and a turbulence intensity of 0.20 (open terrain), a value of 1.77 is calculated for G_u (ESDU 2002). Table 4 shows the G_u values corresponding to different averaging periods calculated according to ESDU (2002).

5.2. Driving rain intrusion

5.2.1. Roof breaches

The volumetric rate of oblique driving rain intrusion (litre/hr) via a roof opening is

$$VOL_R = RAF_R \cdot R_{WDR} \cdot A_{SV} \qquad (9)$$

where RAF_R is the rain admittance factor (Straube & Burnett 2000) for roof which is the ratio of the rainwater intrusion intensity to the free-field WDR intensity, R_{WDR} is the free-field WDR intensity given by Eq. (7), A_{SV} is the vertical projection area of a metal roof sheet opening with $A_{SV} = A_S \sin(\alpha)$, where A_S is the area of the damaged metal sheet and α is the roof slope (21.5° for the representative contemporary house). The RAF_R mainly depends on building geometries and aerodynamics to account for the building disturbance to the free-field WDR.

The RAF_R value is estimated based on limited experimental evidence (Baheru et al. 2014). The RAF_R for roof openings on the windward side is assumed to follow a truncated normal distribution with a mean of 0.30 and a standard deviation of 0.20 (truncated to an interval of 0 to 1), whereas the RAF_R value for roof openings on the leeward side is zero. For roof openings parallel to the wind direction, the RAF_R is assumed to follow a truncated normal distribution with a mean of 0.05 and a standard deviation of 0.05 (truncated to an interval of 0 to 1). For oblique wind angles, it can be approximately accounted for by projecting onto directions normal and parallel to the building facades (Straube & Burnett 2000; Blocken & Carmeliet 2004). As the building geometries and wind conditions in Baheru et al. (2014) do not exactly match those for the representative house examined in this study, a relatively large standard deviation is selected for the truncated normal distribution of RAF_R values to implicitly account for the uncertainties involved. The statistical parameters for RAF_R are summarized in Table 5. There is a clear need to modify the estimation of RAF_R values with more evidence from experiments and/or CFD studies to better inform the semi-empirical model, and hence improve the accuracy of the rainwater intrusion model.

5.2.2. Window breaches

Only the horizontal component of the oblique driving rain enters window breaches. The volumetric rate of driving rain intrusion via a window opening is

$$VOL_W = RAF_W \cdot R_{WDR} \cdot A_W \tag{10}$$

where A_W is the area of the window opening, and RAF_W is the rain admittance factor for window. The value of RAF_W is only non-zero for window openings on the windward wall, which is assumed to follow a truncated normal distribution with a mean of 0.50 and a standard deviation of 0.20 (truncated to an interval of 0 to 1) as inferred from Straube & Burnett (2000) and Baheru et al. (2014) as shown in Table 5. A cosine projection (Straube & Burnett 2000; Blocken & Carmeliet 2004) can be used to approximately account for the rain driven by oblique wind (i.e. wind angle is non-normal to the wall/window).

5.2.3. Gaps around windows

The volumetric rate of driving rain intrusion via gaps around the window is given by

$$VOL_G = f_v \cdot RAF_W \cdot R_{WDR} \cdot A_G \tag{11}$$

where A_G is the area of the gap (mm^2), and f_v is a velocity ratio that accounts for the speed change of air as it passes through small gaps, cracks and openings on buildings (Baheru et al. 2015). As shown in Table 5, the f_v value is assumed to follow a normal distribution with a mean of 2.50 and a standard deviation of 0.30 which is estimated based on the environmental design guide CIBSE (2015) for air infiltration driven by wind through small gaps in buildings. A gap width of 0.5 mm is assumed for windows in the representative contemporary house.

5.3. Rainwater runoff

The rainwater runoff is another source of rainwater intrusion through breaches and gaps in the building envelope. A portion of the oblique driving rain deposited on the upstream undamaged building envelope can run into the damaged roof sheets and windows. The volumetric rate of rainwater runoff into a roof or window opening (VOL_{RO}) is simply calculated by applying a reduction factor, f_r, to the volumetric rate of driving rain impinging on the upstream surface of undamaged building envelope. For example, Fig. 6 shows the upstream runoff surface of a roof opening. This reduction factor accounts for the loss of rainwater amount due to splashing, evaporation, absorption and adhesion, which is assumed to follow a truncated

normal distribution with a mean of 0.25 and a standard deviation of 0.15 (truncated to an interval of 0 to 1) as shown in Table 5. This estimation is based on the engineering judgement that the representative contemporary house only experiences a small portion of runoff water. The basis of this engineering judgement are given herein. A brick veneer wall has great capacity for water absorption to reduce rainwater runoff through windows. Windows on Australian contemporary houses are typically positioned very close to the eave with limited area of upstream surface for rainwater runoff. The corrugation of metal roof sheets reduces rainwater runoff through roof openings. Sensitivity analyses for the factors listed in Table 5 are conducted in Section 7.2.3 to examine their effects on the risk assessment.

5.4. Volumetric rate of rainwater intrusion

A MCS analysis is employed to evaluate the total volumetric rate of rainwater intrusion VOL_T (litre/hr) through roof and window breaches, and gaps around the window (i.e. VOL_R, VOL_W, VOL_G, and VOL_{RO} for all building envelope breaches and gaps). For the dominant opening scenario, the total size of openings due to window breakage on a windward wall is estimated to be $4m^2$. A sensitivity analysis is conducted in Section 7.2.3 for a different opening size. The MCS used for wind fragility analysis is extended to assess the subsequent rainwater intrusion by applying the semi-empirical model. The volumetric rates of rainwater intrusion are dependent on the number and locations of failed roof sheets obtained from the fragility analysis, and also a function of gust wind speed and rainfall intensity.

Figure 7 shows the mean VOL_T for the two wall opening scenarios. As expected, the mean VOL_T increases with wind speed and rainfall intensity. The nonlinearity of rainwater intrusion with increasing wind speed is because there is more roof sheeting loss at a higher wind speed allowing for more rainwater intrusion. Figure 8 shows the mean volumetric rates of rainwater intrusion through roof and window, respectively, under the two wall opening scenarios at a rainfall intensity of 10 mm/hr, which suggests that the rainwater intrusion via window is higher

than that through roof openings for relatively lower wind speeds. With an increasing wind speed, more roof openings tend to occur due to increasing metal roof sheeting loss, which results in more rainwater intrusion via roof openings.

5.5. Volume of rainwater intrusion

The evolution of internal pressurisation and load redistribution due to the progressive failure of the building envelope are explicitly accounted for in the wind damage assessment (see Qin & Stewart 2019 for more details), however, the temporal damage progression of the building envelope is not explicitly considered. It is assumed that the roof damage and the exceedance of limit states for windward windows given by Table 2 all happen at the occurrence time of the maximum gust wind speed (T_M) during a windstorm. The volume of rainwater intrusion (VOL) through all breaches and gaps in the building envelope is then given by

$$VOL = VOL_T \cdot T_R \tag{12}$$

where $T_R = D_{ur} - T_M$ is the length of time after the wind damage to the building envelope, and T_M is assumed to follow a uniform distribution with a lower bound of zero and an upper bound of $D_{ur.}$ Note that VOL_T evaluated in Section 5.4 is based on the average rainfall intensity R_h. This is another approximation that the temporal variation of rainfall intensity during a windstorm is not explicitly taken into account, and hence the assessment of rainwater intrusion volume in this study is not fully event-based.

6. Loss Modelling

6.1. Subassembly cost ratios

The loss estimation uses an assembly-based approach (e.g. Porter et al. 2001; HAZUS 2014; Hamid et al. 2010; Stewart et al. 2018). The entire house is divided into subassemblies/ components based on specific building details. Then the total loss is equal to the sum of repair or replacement costs of every housing components. The loss estimation takes into account housing components/subassemblies that are related to the failure of roof cladding and trusses,

windward windows, and those susceptible to rainwater damage. The representative contemporary house described in Section 4.1 is then divided into subassemblies as shown in Table 6. The subassemblies (e.g. site preparations, foundations, wall structures, etc.) that are not explicitly included in the loss estimation are categorized under 'other'.

The losses are estimated in terms of cost ratios. Herein, the cost ratio of a subassembly is defined as the ratio of the cost to complete the subassembly (i.e. newly build, upgrade, repair or replace) to the building value. The estimated total cost to build a new contemporary house with an approximate floor area of 150 m^2 is $L_{building}$ = \$300,000 Australian Dollars (HIA 2018 and RLB 2019). Based on cost data provided by Australian housing cost guides (Rawlinsons 2015) and subjective judgement, the subassembly cost ratios are estimated for a representative contemporary house built to an average standard as shown in Table 6. Note that the cost ratios in Table 6 are estimated for new construction that includes material and labour costs plus contractor's overhead and profit. In the context of this study, cost ratios for repair and/or replacement of damaged components/subassemblies are needed, which can be obtained by adjusting the cost ratios in Table 6 using a factor of 1.25 to account for the additional costs associated with removal, repair and remodelling of an existing house (HAZUS 2014), and a factor of 1.05 to account for increased contractor's overhead and profit for repair and/or replacement work (Rawlinsons 2015). The adjusted cost ratios are also given in Table 6.

6.2. Loss functions

6.2.1. Roof cladding loss

Insurance data in Australia suggests that the metal roof is likely to be entirely replaced if the proportion of roof sheeting damage exceeds 20% (Smith & Henderson 2015), hence,

$$\Pr(L_1|DS = R_{clad}) = \begin{cases} R_{clad} & R_{clad} \leq 20\% \\ 1.0 & R_{clad} > 20\% \end{cases} \tag{13}$$

where R_{clad} is the proportion of metal roof cladding damage and L_1 = 5.4% is the cost ratio for

full replacement of roof cladding.

6.2.2. Roof framing loss

The cost ratio for a full roof framing replacement is $L_2 = 20.9\%$. The roof framing includes timber roof trusses, jack and hip rafters, ridgeboard, valley rafters, struts and ties, ceiling joists, fixings and connections, etc. In the wind fragility assessment, only the failures of critical roof trusses are explicitly evaluated. It is assumed that the failure of a critical truss causes damage to other framing elements directly and/or indirectly linked to this truss. In this study, a threshold value of 20% is assumed for a full replacement of the roof framing based on existing loss functions and damage states used in the literature (e.g. van de Lindt & Dao 2012; Li et al. 2011). In other words, if the damage proportion of the critical roof trusses exceeds this threshold value, a full replacement of the entire roof framing is then required, leading to

$$\Pr(L_2|DS = R_{truss}) = \begin{cases} R_{truss} & R_{truss} \leq 20\% \\ 1.0 & R_{truss} > 20\% \end{cases} \tag{14}$$

where R_{truss} is the damage proportion of the critical roof trusses.

6.2.3. Windward windows

The ratio of windward window loss caused by high wind pressure is expressed as

$$\Pr(L_3|DS) = \begin{cases} 0 & W_{win} < R_{ult} \\ 1.0 & W_{win} \geq R_{ult} \end{cases} \tag{15}$$

where $L_3 = 1.0\%$.

6.2.4. Interior loss

The building interior considered in the loss estimation includes internal finishes and fittings, mechanical and electrical systems. The cost ratio for a full replacement of interior is $L_4 = 51.2\%$. The interior loss is modelled as a function of rainwater intrusion, and it is assumed that the interior losses increase linearly with an increasing amount of rainwater intrusion until

exceeding a threshold value to cause a complete loss (Pita et al. 2012; HAZUS 2014). The proportion of interior loss due to rainwater damage is

$$\Pr(L_4|DS = h_I) = \begin{cases} \frac{h_I}{h_T} & h_I \le h_T \\ 1.0 & h_I > h_T \end{cases} \tag{16}$$

where h_I (mm) is the accumulated water depth calculated as the total rainwater intrusion volume VOL given by Eq. (12) divided by the floor area of the entire house, and h_T (mm) is a threshold value of water depth that leads to total interior loss. A threshold value of $h_T = 25$ mm given by Pita et al. (2012) is used in this study. A sensitivity analysis for h_T is presented in Section 7.2.3 to examine its effect on annual expected losses.

6.2.5. Contents loss

The contents loss is also modelled as a function of rainwater intrusion. The contents loss is directly related to rainwater entering from windows, and it is assumed that the contents can only be damaged by rainwater entering from the roof if the ceiling leaks (e.g. due to local damage of a ceiling). In this case, a weighting factor, $w_0 = 0.6$, is assumed for the proportion of water depth resulting from a damaged roof that causes contents loss. A sensitivity analysis is conducted in Section 7.2.3 for this weighting factor. Using the same threshold value of water depth, $h_T = 25$ mm, the proportion of contents loss due to rainwater damage is

$$\Pr(L_5|DS = w_0 h_R + h_W) = \begin{cases} \frac{w_0 h_R + h_W}{h_T} & w_0 h_R + h_W \le h_T \\ 1.0 & w_0 h_R + h_W > h_T \end{cases} \tag{17}$$

where h_R and h_W are the accumulated water depth due to rainwater intrusion via roof and windows, respectively. Based on the statistics of the average value of a household's home contents in Australia (ABS 2011), it is estimated that $L_5 = 25.0\%$.

6.2.6. Loss of use

The annual probability of loss of use due to housing damage is (HAZUS 2014)

$$\Pr(L_6|DS) = \frac{\text{N}_{\text{lou}}\big(\Pr(L_{building}|DS)\,L_{building}\big)\cdot\text{Mod}\big(\Pr(L_{building}|DS)\,L_{building}\big)}{365} \qquad (18)$$

where N_{lou} is the loss of use (days) accounting for delays in decision-making, financing, inspection, etc., and Mod is a multiplier to account for the fact that the house can still be occupied if damage is not severe (HAZUS 2014). Both N_{lou} and Mod are modelled as a function of the expected total building loss, i.e. $\Pr(L_{building}|DS)L_{building}$, which is a summation of all the subassembly losses (excluding contents loss) considered in this study (i.e. $\sum_{i=1}^{4} \Pr(L_i|DS)\,L_i$). Detailed values for N_{lou} and Mod can be found in HAZUS (2014) and Stewart et al. (2018). The annual loss of use (365 days) corresponds to a cost ratio of $L_6 = 16.3\%$ based on an estimated additional living cost of \$1,000 per week (e.g. rent, hotel costs, relocation and increased transportation fees, furniture rental costs, etc.).

7. Economic Losses and Risks

7.1. Risk analysis method

The annual risk (expressed as the expected loss) is given by

$$E_{annual}(L) = \int_0^\infty \int_0^\infty \int_0^\infty f(R_h \,|\, v, D_{ur}) f(v) f(D_{ur}) \frac{1}{n_d} \sum_{j=1}^{n_d} \left[\Pr(DS \,|\, D_{Nj} T_N v, R_h, D_{ur}) \sum_{i=1}^{n_c} \Pr(L_i \,|\, DS) L_i \right] dv \, dR_h \, dD_{ur} \qquad (19)$$

where $f(v)$ is the probability distribution of the annual maximum gust wind speed, $f(R_h\,|\,v, D_{ur})$ is the probability distribution of the average rainfall intensity of a severe windstorm corresponding to a given duration D_{ur}, $f(D_{ur})$ is the probabilistic distribution of the windstorm duration, $n_d = 8$ is the number of cardinal wind directions considered in this study, $n_c = 6$ is the number of subassemblies/components considered in the loss estimation as described in Section 6, D_N is the nominal wind directionality factor for eight cardinal directions, and T_N is the nominal value of the shielding factor, $\Pr(DS\,|\,v, R_h, D_{ur})$ is the likelihood of damage state (e.g. extent of roof damage, amount of rainwater intrusion) given the gust wind speed, rainfall intensity and storm duration, $\Pr(L_i\,|\,DS)$ is the loss likelihood for the ith component/subassembly

described in Section 6.2, and L_i is the maximum probable loss for the ith subassembly/component.

The probabilistic models for $f(v)$, $f(D_{ur})$ and $f(R_h | v, D_{ur})$ are described in Section 3. The D_N and T_N values are obtained from AS/NZS 1170.2 (2011) for suburban houses in Brisbane and Melbourne with different site conditions and design wind classifications (see Table 7). Note that Eq. (19) assumes that damage is caused by the largest windstorm in any calendar year, which slightly underestimates the risks due to the ignorance of less severe windstorms in the same year. An alternative way is the adoption of a Poisson distribution to model the number of severe windstorms in a calendar year, and a Generalized Pareto distribution for the maximum gust wind speed in each windstorm (i.e. method of 'peaks over threshold'). This is subjected to further examination if more meteorological data are accessible.

The probabilistic risk assessment conducted using a MCS analysis consists of four major components, i.e. (i) hazard modelling for wind and rainfall, (ii) reliability-based wind damage assessment, (iii) evaluation of rainwater intrusion, and (iv) loss estimation. Figure 9 shows an outline to illustrate the risk analysis method to assess the annual expected economic losses for the representative contemporary house subjected to non-cyclonic extreme winds and associated rainfall.

7.2. Results

The risk analysis is conducted for the representative contemporary house built in suburbs of Brisbane and Melbourne. The CTB and BTR connections are considered to be identical for houses with different design wind classifications, whereas the RTW connections and window strengths are different. The higher the design wind classification, the stronger the RTW connections and windows (i.e. with higher ultimate strength against wind pressure). However, this is not the case for the water penetration resistance of windows (see Table 1).

7.2.1. Annual expected losses

Table 8 shows the total annual expected losses (normalized by the building value) including the loss of use (i.e. L_6). The annual expected losses to each housing component/subassembly (L_1 to L_5 described in Section 6.2), the average days for loss of use in a calendar year and the proportion of window breakage (i.e. dominant opening scenario) are also given in Table 8. As shown in this table, building interior and contents losses are the major contributor to the annual risks (i.e. more than 90% of the total building loss), which is much larger than the direct losses to metal roof cladding, timber roof framing and windward windows. This is because the annual expected damage proportions of roof and windows are small. In addition, the costs to repair or replace roof and windows are much less than those for building interior and contents. Although the economic losses directly caused by roof sheeting loss and window breakage are not significant, a small portion of such building envelope breaches may induce significant losses to building interior and contents due to rainwater intrusion.

As indicated in Table 8, window breakage is rare, and hence the non-dominant opening scenario is more likely to occur. Since the proportion of roof sheeting loss is small under the non-dominant opening scenario as shown in Fig. 5(a), in most cases, more rainwater enters through gaps around windward windows when the water penetration resistance is exceeded (see Fig. 8). For example, the Brisbane house with a wind classification of N2 suffers more losses from rainwater intrusion than the house with a wind classification of N3, mainly due to a lower water penetration resistance of the windward wall window (see Table 1). Melbourne houses with a design wind classification of N2 are subjected to higher wind pressure than those with a design wind classification of N1 but the water penetration resistances of the windward window are comparable. This results in slightly higher building interior and contents losses for Melbourne houses with a design wind classification of N2. Table 8 also indicates that houses in Brisbane are generally subjected to higher losses than houses in Melbourne because the

extreme wind speed and rainfall intensity are higher in Brisbane, though Brisbane houses have been designed to resist higher wind speed. Note that the annual risks presented in Table 8 may be used as a lower bound. Construction defects are common in housing construction, which can increase the roof damage and also subsequently incur more rainwater damage. Incorporation of the construction defects in the risk analysis will be conducted in a future study. Moreover, window breakage by windborne debris can be further incorporated if a residential community is considered.

Table 9 shows the mean proportions of wind damage to metal roof cladding and timber roof trusses, and the mean depth of rainwater intrusion at the 50-year and 500-year gust wind speed (i.e. V_{50} and V_{500}). Table 9 suggests that the metal roof cladding and timber roof trusses are subjected to negligible damage at the 50-year wind speed, which is expected. At the wind speed $V_{50} = 35$ m/s for Melbourne and $V_{50} = 43$ m/s for Brisbane, houses are more likely under the non-dominant opening scenario, and the proportions of roof sheeting loss and roof truss failures are close to zero (see Fig. 5). The losses at V_{50} are mainly due to the rainwater intrusion through gaps around windward windows. At the 500-year wind speed, Brisbane houses with a design wind classification of N2 are subjected to more damage to roof trusses than those with a design wind classification of N3, because the former has weaker RTW connections (see Fig. 5b). Slight roof truss damage is predicted for Melbourne houses at V_{500}. The amount of rainwater intrusion increases at V_{500} due to the increasing building envelope breaches and wind speed.

7.2.2. Implications for insurance premium

According to Goda & Hong (2008), the annual insurance premium (*INP*) charged by an insurer for a building is

$$INP = (1 + \eta) \cdot E[I(ML)] \tag{20}$$

where *E[I(ML)]* is the annual expected value of indemnity *I(ML)*, and η is the insurance loading factor. As inferred from Walker et al. (2016), η is typically greater than 0.3 to account for

administration costs and profits, and could be considerably large for high exposure areas. The indemnity $I(ML)$ is expressed as a function of the monetary loss ML (Goda & Hong 2008), given by

$$I(ML) = \begin{cases} 0 & ML \leq EX \\ CO \cdot (ML - EX) & EX < ML < INV \\ CO \cdot (INV - EX) & ML \geq INV \end{cases} \tag{21}$$

where CO is the co-insurance factor that typically equals to 1.0 for home insurance in Australia, EX is the excess fee or deductibles, and INV is the insured value of the house. If EX equals to zero and INV is infinity, $E[I(ML)]$ is the annual expected loss given by Table 8.

For a typical building and contents insurance policy for the representative contemporary house described in Section 4.1 with a EX of $600, the annual insurance premium INP ranges from $1,000 to $1,500 for houses in Brisbane and $600 to $1,000 for houses in Melbourne, which includes risks from windstorms, theft, impact, earthquake, fire, accidental damage, etc. The flood coverage is generally optional and not initially included in INP. It is further assumed that INV is 30% higher than the total building and contents value (i.e. $375,000 as described in Section 6). By substituting the random samples of ML yielded by the probabilistic risk assessment using MCS analysis into Eq. (21), $E[I(ML)]$ is estimated to be $257 and $206 for the Brisbane house with a design wind classification of N2 and N3, respectively. For the Melbourne house with a design wind classification of N1 and N2, $E[I(ML)]$ is estimated to be $76 and $101, respectively. These estimates seem to be reasonable risk premiums for wind and rainfall damage compared to the typical INP values for Brisbane and Melbourne houses including all sources of risks. Incorporating the effects of construction defects can further increase the estimates. A detailed reality check can be further conducted if the breakdown of a typical insurance premium for housing (e.g. annual premiums respectively correspond to distinct natural and man-made hazards) is known.

7.2.3. Sensitivity analysis

7.2.3.1. Parameters of rainwater intrusion model

The parameters of the semi-empirical rainwater intrusion model given by Table 5 are subjected to considerable uncertainties due to limited experimental and field monitoring evidence. A sensitivity analysis is conducted by varying the mean values of the parameters in Table 5 by ±50% and adjusting the corresponding standard deviations accordingly to keep the COV values unchanged. Table 10 shows the respective effects of RAF_R, RAF_W, f_v and f_r on the annual expected losses. The variations of the mean RAF_R and f_v have limited effects on the estimated annual expected losses, whereas the risk analysis is relatively sensitive to changes in RAF_W, which indicates that rainwater tends to enter from windward windows. Varying the mean f_r considerably changes the estimated annual expected losses by up to 10%, and hence more detailed evaluation of rainwater runoff by either experiments or numerical methods (e.g. Blocken & Carmeliet 2012; Blocken & Carmeliet 2015) for the building material of the representative contemporary house are needed to better estimate this reduction factor in the future work.

7.2.3.2. Parameters in loss functions

The threshold of water depth h_T leading to a total loss of building interior and contents, and the weighting factor w_0 in Eq. (16) and (17) are varied by ±50%. The corresponding changes in the calculated annual expected losses are also shown in Table 10. While the effect of w_0 is negligible, the estimated annual expected losses are very sensitive to a −50% decrease in h_T. This threshold value may depend on the materials of building interior and contents as well as many local factors in pricing and claim evaluation. Hence, a revision of h_T is needed if relevant insurance data in Australia becomes available and accessible.

7.2.3.3. Window size and resistance

A sensitivity analysis suggests that the annual expected losses increase by up to 70% if the

windward window area (A_W) is doubled to 8m^2 as also shown in Table 10. Therefore, a contemporary house with a higher window-to-floor ratio (i.e. window area divided by the floor area, typically less than 25% for Australian housing) is more susceptible to wind and rain losses. However, the determination of window-to-floor ratio depends on many other factors such as natural lighting, ventilation, energy efficiency and architectural appearance, etc.

The mean window resistances (i.e. R_{ult} and R_{water}) given by Table 1 are varied by ±20%. Table 10 shows the sensitivity of the risk analysis to the changes in window resistances. The annual expected losses for Melbourne houses are relatively less sensitive to a 20% change in window resistances and it implies that strengthening windows for housing in Brisbane offers more reduction in economic losses due to extreme wind and associated rainfall.

8. Conclusions and Future Work

In this study, a probabilistic risk assessment framework was developed to evaluate the wind and rain losses for metal-clad houses in non-cyclonic regions of Australia. The components included are (i) a hazard model accounting for the simultaneous occurrence of extreme wind and associated rainfall, (ii) a reliability-based wind damage assessment, (iii) a semi-empirical model for rainwater intrusion, and (iv) a loss estimation model. The risk analysis results suggest that the annual expected losses are mainly attributed to the rainwater damage to building interior and contents. Although houses in Brisbane have a stronger design, they are generally subjected to higher losses than Melbourne houses because the extreme wind speed and associated rainfall intensity are higher in Brisbane.

The current risk assessment is conducted for houses with an idealized construction quality. The effect of construction error (e.g. defects in roof connections, the installed window with an unsatisfied window rating) on the economic losses needs to be further investigated. The parameters of the semi-empirical rainwater intrusion model need a revisit when more experimental evidence and CFD studies are available. The threshold of water depth leading to

a total loss of building interior and contents used in the loss functions can be further modified when more field observations and insurance data are available. Further decision-analysis for risk mitigation can be conducted based on the probability risk assessment in this study.

Acknowledgement

References

ABS (2011). *Australian Social Trends December 2011: Components of household wealth*. Australian Bureau of Statistics, Canberra, Australia.

AS 2047 (2014). *Windows and external glazed doors in buildings*. Standards Australia, Sydney.

AS 4055 (2012). *Wind Loads for Housing*. Standards Australia, Sydney.

AS/NZS 1170.2 (2011). *Structural Design Actions, Part 2: Wind Actions*. Standards Australia, Sydney.

Baheru, T., Chowdhury, A. G., Pinelli, J. P., & Bitsuamlak, G. (2014). Distribution of wind-driven rain deposition on low-rise buildings: Direct impinging raindrops versus surface runoff. *Journal of Wind Engineering and Industrial Aerodynamics*, 133, 27-38.

Baheru, T., Chowdhury, A. G., & Pinelli, J. P. (2015). Estimation of wind-driven rain intrusion through building envelope defects and breaches during tropical cyclones. *Natural Hazards Review*, 16(2), 04014023.

Blocken, B., & Carmeliet, J. (2002). Spatial and temporal distribution of driving rain on a low-rise building. *Wind and Structures*, 5(5), 441-462.

Blocken, B., & Carmeliet, J. (2004). A review of wind-driven rain research in building science. *Journal of wind engineering and industrial aerodynamics*, 92(13), 1079-1130.

Blocken, B., & Carmeliet, J. (2010). Overview of three state-of-the-art wind-driven rain assessment models and comparison based on model theory. *Building and Environment*, 45(3), 691-703.

Blocken, B., & Carmeliet, J. (2012). A simplified numerical model for rainwater runoff on building facades: possibilities and limitations. *Building and Environment*, 53, 59-73.

Blocken, B., & Carmeliet, J. (2015). Impact, runoff and drying of wind-driven rain on a window glass surface: numerical modelling based on experimental validation. *Building and Environment*, 84, 170-180.

Choi, E. C. C. (1994a). Determination of wind-driven-rain intensity on building faces. *Journal of Wind Engineering and Industrial Aerodynamics*, 51(1), 55-69.

Choi, E. C. C. (1994b). Characteristics of the co-occurrence of wind and rain and the driving-rain index. *Journal of wind engineering and industrial aerodynamics*, 53(1-2), 49-62.

CIBSE (2015). *GVA/15 CIBSE Guide A: Environmental Design 2015*. The Chartered Institution of Building Services Engineers, London, UK.

CTS (2018). *North Queensland Study into Water Damage from Cyclones*. A summary of report TS1124, Cyclone Testing Station, James Cook University.

Dao, T. N. (2010). *The development of performance-based wind engineering for residential structures: From concept to application*. Ph.D. dissertation, Colorado State University, Fort Collins, CO, USA.

Dao, T. N., & van de Lindt, J. W. (2010). Methodology for wind-driven rainwater intrusion fragilities for light-frame wood roof systems. *Journal of Structural Engineering*, 136(6), 700-706.

Eagleson, P. S. (1972). Dynamics of flood frequency. *Water Resources Research*, 8(4), 878-898.

ESDU (2002). *Strong winds in the atmospheric boundary layer. II: Discrete gust speeds*. Engineering Science Data Unit, Item No. 83045, London, UK.

Ginger, J., Henderson, D., Edwards, M. and Holmes, J. (2010). Housing damage in windstorms and mitigation for Australia. *Proceedings of 2010 APEC-WW and IG-WRDRR Joint Workshop: Wind-Related Disaster Risk Reduction Activities in Asia-Pacific Region and Cooperative Actions*, 1-18.

Goda, K., & Hong, H. P. (2008). Implied preference for seismic design level and earthquake insurance. *Risk Analysis: An International Journal*, 28(2), 523-537.

Hamid, S., Kibria, B. G., Gulati, S., Powell, M., Annane, B., Cocke, S., ... & Chen, S. C. (2010). Predicting losses of residential structures in the state of Florida by the public hurricane loss evaluation model. *Statistical methodology*, 7(5), 552-573.

HAZUS (2014). *Multi-hazard Loss estimation methodology - hurricane model*. Hazus-MH 2.1 Technical Manual, Federal Emergency Management Agency, Mitigation Division, Washington, DC.

Henderson, D. J., & Ginger, J. D. (2007). Vulnerability model of an Australian high-set house subjected to cyclonic wind loading. *Wind and Structures*, 10(3), 269-285.

Henderson, D., & Ginger, J. (2008). Role of building codes and construction standards in windstorm disaster mitigation. *Australian Journal of Emergency Management*, 23(2), 40-46.

Henderson D, Smith D, Boughton G, Falck D and Ginger J (2017). Damage and losses in engineered buildings from wind and rain. *24th Australasian Conference on the Mechanics of Structures and Materials*. 6-9 December 2016, Perth, Australia.

Heneker, T. M., Lambert, M. F., & Kuczera, G. (2001). A point rainfall model for risk-based design. *Journal of Hydrology*, 247(1-2), 54-71.

HIA (2018). *Window into Housing 2018*. The Housing Industry Association, Canberra, Australia.

ISO (2009). *Hygrothermal performance of buildings – calculation and presentation of climatic data – Part 3: calculation of a driving rain index for vertical surfaces from hourly wind and rain data*. International Organization for Standardization 2009, 15927-3.

Johnson, T., Pinelli, J. P., Baheru, T., Chowdhury, A. G., Weekes, J., & Gurley, K. (2018). Simulation of Rain Penetration and Associated Damage in Buildings within a Hurricane Vulnerability Model. *Natural Hazards Review*, 19(2), 04018004.

Koutsoyiannis, D., & Foufoula-Georgiou, E. (1993). A scaling model of a storm hyetograph. *Water Resources Research*, 29(7), 2345-2361.

Koutsoyiannis, D., Onof, C., & Wheater, H. S. (2003). Multivariate rainfall disaggregation at a fine timescale. *Water Resources Research*, 39(7).

Lambert, M., & Kuczera, G. (1998). Seasonal generalized exponential probability models with application to interstorm and storm durations. *Water Resources Research*, 34(1), 143-148.

Leitch C, Ginger J, Harper B, Kim P, Jayasinghe N, Somerville L (2009). *Investigation of performance of housing in Brisbane following storms on 16 and 19 November 2008*, Technical Report No. 55. Cyclone Testing Station, James Cook University.

Li, Y., van de Lindt, J. W., Dao, T., Bjarnadottir, S., & Ahuja, A. (2011). Loss analysis for combined wind and surge in hurricanes. *Natural hazards review*, 13(1), 1-10.

Mudd, L., Rosowsky, D., Letchford, C., & Lombardo, F. (2016). Joint Probabilistic Wind–Rainfall Model for Tropical Cyclone Hazard Characterization. *Journal of Structural Engineering*, 143(3), 04016195.

Pant, S., & Cha, E. J. (2019). Wind and rainfall loss assessment for residential buildings under climate-dependent hurricane scenarios. *Structure and Infrastructure Engineering*, 15(6), 771-782.

Parackal, K. I., Humphreys, M. T., Ginger, J. D., & Henderson, D. J. (2016). Wind Loads on Contemporary Australian Housing. *Australian Journal of Structural Engineering*, 17(2), 136-150.

Pita, G., Pinelli, J. P., Cocke, S., Gurley, K., Mitrani-Reiser, J., Weekes, J., & Hamid, S. (2012). Assessment of hurricane-induced internal damage to low-rise buildings in the Florida Public Hurricane Loss Model. *Journal of Wind Engineering and Industrial Aerodynamics*, 104, 76-87.

Porter, K. A., Kiremidjian, A. S., & LeGrue, J. S. (2001). Assembly-based vulnerability of buildings and its use in performance evaluation. *Earthquake spectra*, 17(2), 291-312.

Qin, H., & Stewart, M. G. (2019). System fragility analysis of roof cladding and trusses for Australian contemporary housing subjected to wind uplift. *Structural Safety*, 79, 80-93.

R Core Team (2019). *R: A language and environment for statistical computing*. R Foundation for Statistical Computing, Vienna, Austria. URL: http://www.R-project.org/.

Rawlinsons (2015). *Rawlinsons Construction Cost Guide 2015*. Rawlinsons Publishing, Perth, Australia.

RLB (2019). *Riders Digest* 47th *Edition*. Rider Levett Bucknall, Australia.

Smith, D., & Henderson, D. (2015). *Suncorp group limited: Cyclone resilience research – Phase II*. Report TS1018, Cyclone Testing Station, James Cook University, Australia.

Stewart, M. G., Ginger, J. D., Henderson, D. J., & Ryan, P. C. (2018). Fragility and climate impact assessment of contemporary housing roof sheeting failure due to extreme wind. *Engineering Structures*, 171, 464-475.

Straube, J. F., & Burnett, E. F. P. (2000). Simplified prediction of driving rain on buildings. *Proceedings of the international building physics conference*. Eindhoven, Netherlands.

van de Lindt, J. W., & Nguyen Dao, T. (2012). Loss analysis for wood frame buildings during hurricanes. II: Loss estimation. *Journal of performance of constructed facilities*, 26(6), 739-747.

Walker, G. R., Mason, M. S., Crompton, R. P., & Musulin, R. T. (2016). Application of insurance modelling tools to climate change adaptation decision-making relating to the built environment. *Structure and Infrastructure Engineering*, 12(4), 450-462.

Wang, C. H., Wang, X., & Khoo, Y. B. (2013). Extreme wind gust hazard in Australia and its sensitivity to climate change. *Natural hazards*, 67(2), 549-567.

Tables

Table 1. Ultimate strength and water penetration resistance of windows.

Window rating	R_{ult} (Pa)		R_{water} (Pa)		Distribution type
	Mean	COV	Mean	COV	
N1	720	0.20	180	0.20	
N2	1080	0.20	180	0.20	Normal
N3	1680	0.20	360	0.20	

Table 2. Limit states for the windward window.

Limit states	Internal pressurisation scenario	Water entry
$W_{win} \geq R_{ult}$	Windward dominant opening	Via window breakage
$W_{win} \geq R_{water} \cap W_{win} < R_{ult}$	No dominant opening	Via small gaps around the window
$W_{win} < R_{water}$	No dominant opening	No entry via window

Table 3. *DRF* values corresponding to various rainfall intensities.

R_h (mm/hr)	10	20	30	40	50	60	80	100
DRF	0.209	0.186	0.175	0.168	0.163	0.159	0.153	0.149

Table 4. Gust factors corresponding to different averaging periods (gust duration of 0.2s).

Averaging periods (hr)	0.5	1	2	3	6	9	12	18	24
Gust factor (G_u)	1.73	1.77	1.80	1.82	1.85	1.87	1.88	1.90	1.91

Table 5. Random variables in the semi-empirical rainwater intrusion model.

Parameters	Location applied	Mean	Standard deviation	Distribution	Source
RAF_R	Windward roof	0.30	0.20	Truncated normal[a]	Inferred from Baheru et al. (2014)
	Sideward roof	0.05	0.05		
	Leeward roof	0.00	0.00		
RAF_W	Windward window	0.50	0.20	Truncated normal[a]	Inferred from Straube & Burnett (2000) Baheru et al. (2014)
f_v	Gaps around windward window	2.50	0.30	Truncated normal[a]	Inferred from CIBSE (2015)
f_r	Upstream undamaged surface	0.25	0.15	Truncated normal[a]	Assumed based on engineering judgement

[a]Truncated to an interval of 0 to 1.

Table 6. Subassembly cost ratios for the representative contemporary house.

Subassembly		Description	Cost ratio	Adjusted cost ratio
Roof	Roof cladding	Mainly including corrugated metal sheets, metal battens and insulation	4.1%	$L_1 = 5.4\%$
	Roof framing	Timber trusses, rafters, ceiling joists, fixings, etc.	15.9%	$L_2 = 20.9\%$
Windows on one wall		Single glazed, aluminum sliding or awning windows	0.8%	$L_3 = 1.0\%$
Internal finishes, fittings	Wall	Mostly plasterboard, also include ceramic tiles and painting	6.8%	$L_4 = 51.2\%$ (building interior)
	Floor	Mixed use of timber, carpet and ceramic tiles	3.5%	
	Ceiling	Mostly plasterboard, also including painting	4.7%	
	Fittings and fixtures	Built-in wardrobes/cupboards, kitchen units, bathroom suites, shelving, internal doors, etc.	10.0%	
Mechanical		Air conditioning, heaters, ventilation, etc.	10.0%	
Electrical		Lighting, conduits, cables, etc.	4.0%	
Other		Site preparation, foundation, wall framing, other fenestrations, plumbing, etc.	37.0%	n/a

Table 7. Nominal values of T and D for suburban houses with different design wind classifications.

	Design wind classification	T_N	D_N
Brisbane house	N2	0.90	1.0
	N3	1.0	1.0
Melbourne house	N1	0.90	See Table 3.2 in
	N2	1.0	AS/NZS 1170.2 (2011)

Table 8. Annual expected losses for the representative contemporary house.

	Design wind classification	Annual expected loss (%)						Loss of use (days)	Portion of window breakage (%)
		L_1	L_2	L_3	L_4	L_5	Total		
Brisbane	N2	0.004	0.003	0.003	0.069	0.030	0.109	0.22	0.27
	N3	0.006	0.002	0.001	0.053	0.023	0.085	0.17	0.07
Melbourne	N1	0.000	0.000	0.000	0.024	0.011	0.035	0.04	0.009
	N2	0.000	0.000	0.000	0.032	0.014	0.046	0.06	0.006

Table 9. Mean damage states under extreme wind speed with 50 and 500 year return periods.

	Design wind classification	V_{50}			V_{500}		
		R_{clad} (%)	R_{truss} (%)	h_I (mm)	R_{clad} (%)	R_{truss} (%)	h_I (mm)
Brisbane house	N2	0.00	0.00	0.10	0.73	1.01	0.22
	N3	0.00	0.00	0.08	1.22	0.56	0.16
Melbourne house	N1	0.00	0.00	0.02	0.00	0.00	0.04
	N2	0.00	0.00	0.03	0.00	0.00	0.05

Table 10. Sensitivity of annual expected losses to various uncertain parameters.

Parameters	Variations for sensitivity analysis	Approximate changes in annual expected losses	
		Brisbane house	Melbourne house
RAF_R	±50% of the mean values given in Table 5 and COV values unchanged	±5%	±5%
RAF_W		±30%	±30%
f_v		±1%	±1%
f_r		±10%	±40%
h_T	±50% of the values given in Section 6.2.4 and 6.2.5	−30% and +60%	−30% and +70%
w_0		±1%	±1%
A_W	Doubled to 8m^2	+70%	+70%
R_{ult} and R_{water}	±20% of the mean window resistances given in Table 1	−20% and +25%	−10% and +15%

Figures
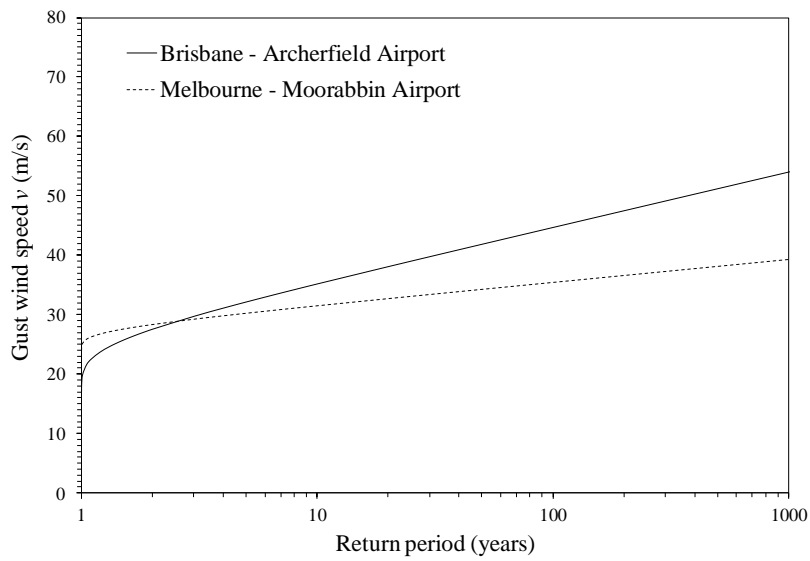
Figure 1. Extreme gust wind speed corresponding to return periods.
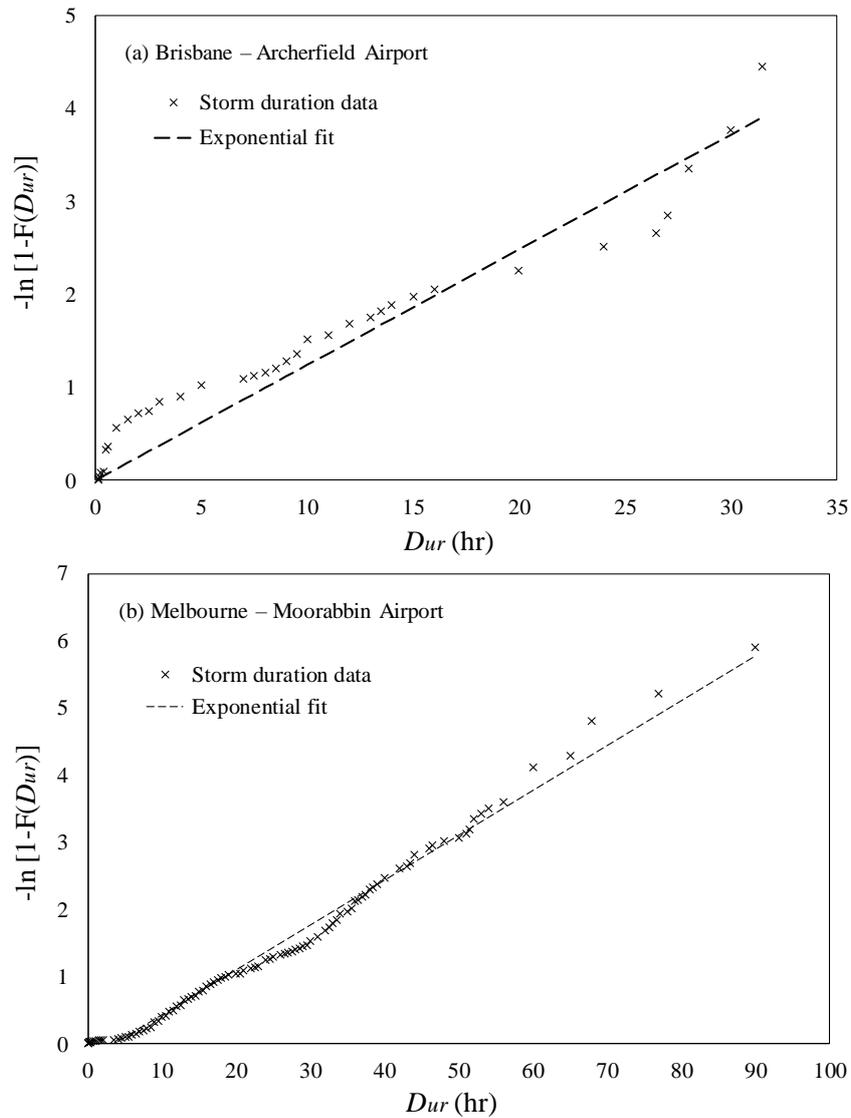
Figure 2. Exponential probability plots for storm duration D_{ur}.
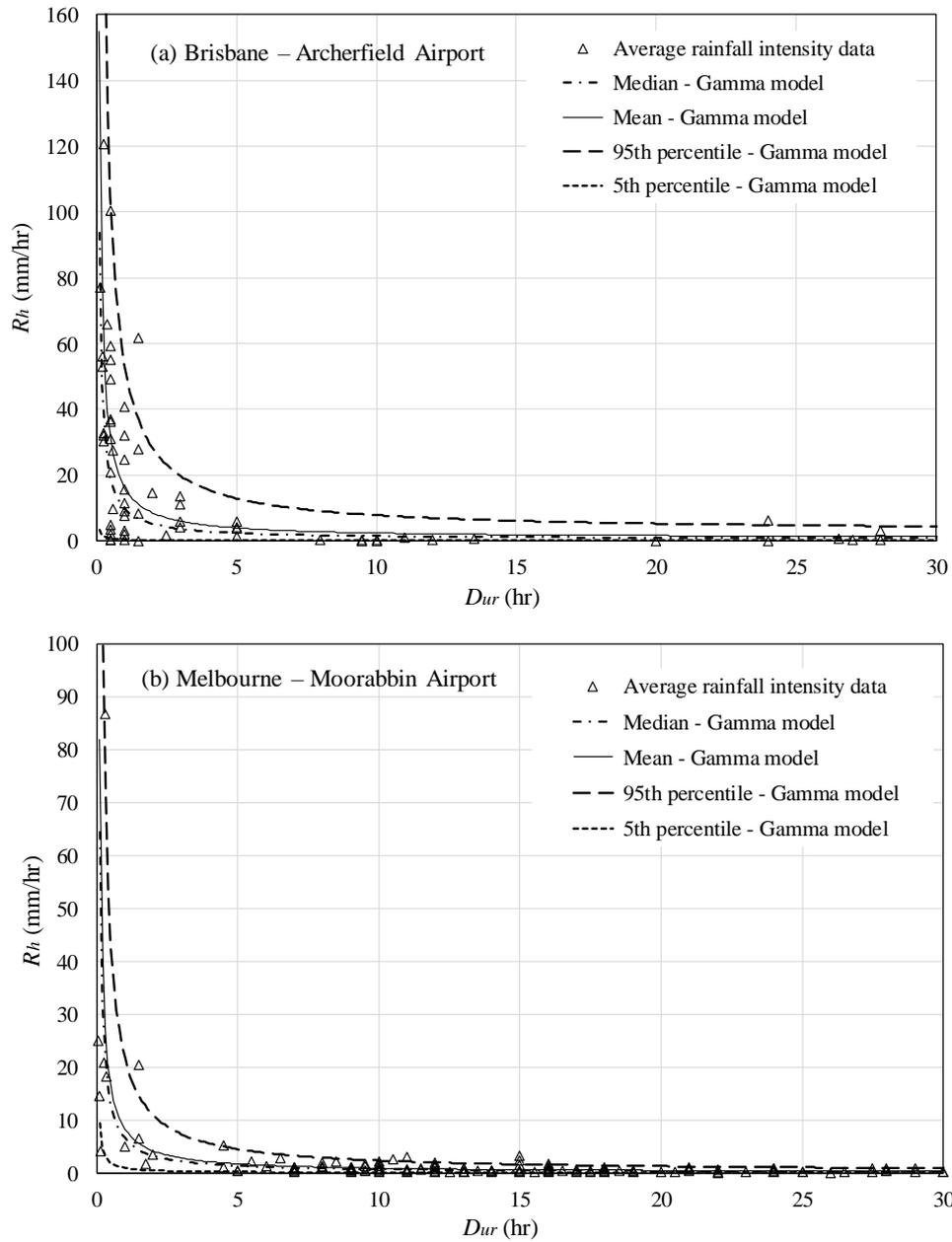
Figure 3. Average rainfall intensity R_h from the observed data and gamma regression model.

(a) 3D view   (b) Plan view
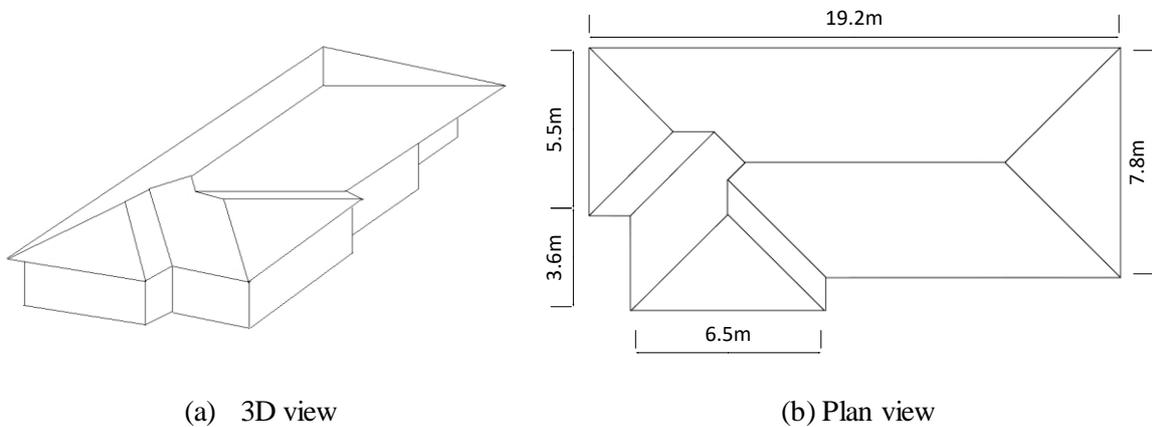
Figure 4. One-storey representative contemporary house.
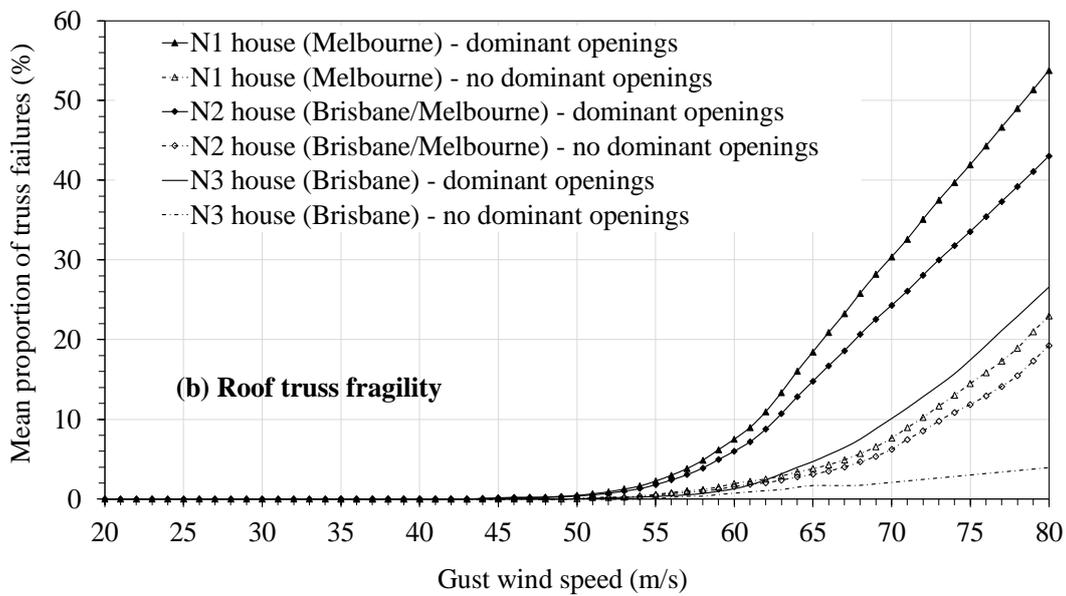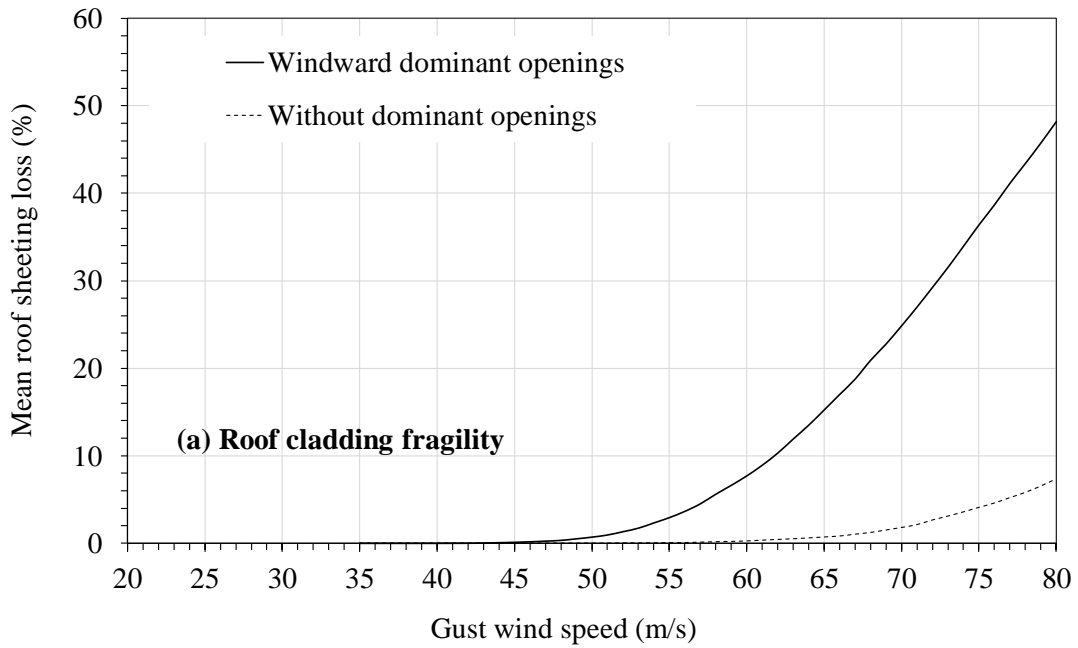
Figure 5. Fragility curves for metal roof cladding and timber roof trusses.
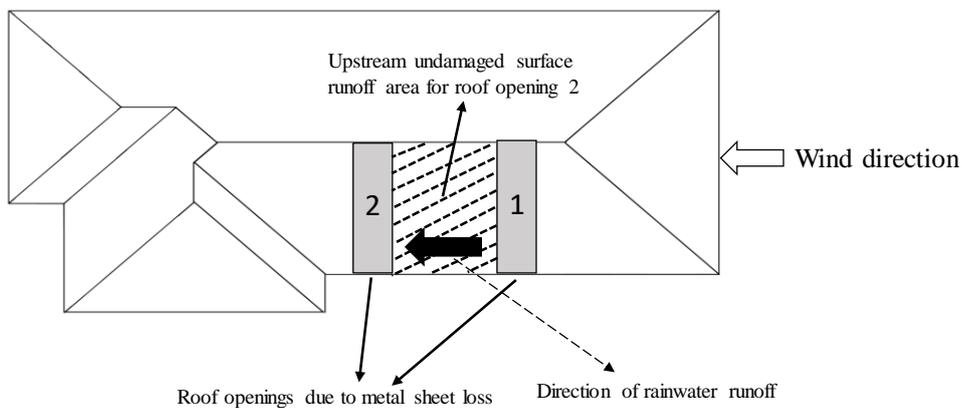
Figure 6. Upstream undamaged surface runoff area for a roof opening due to metal sheet loss.

(a) Windward wall dominant openings
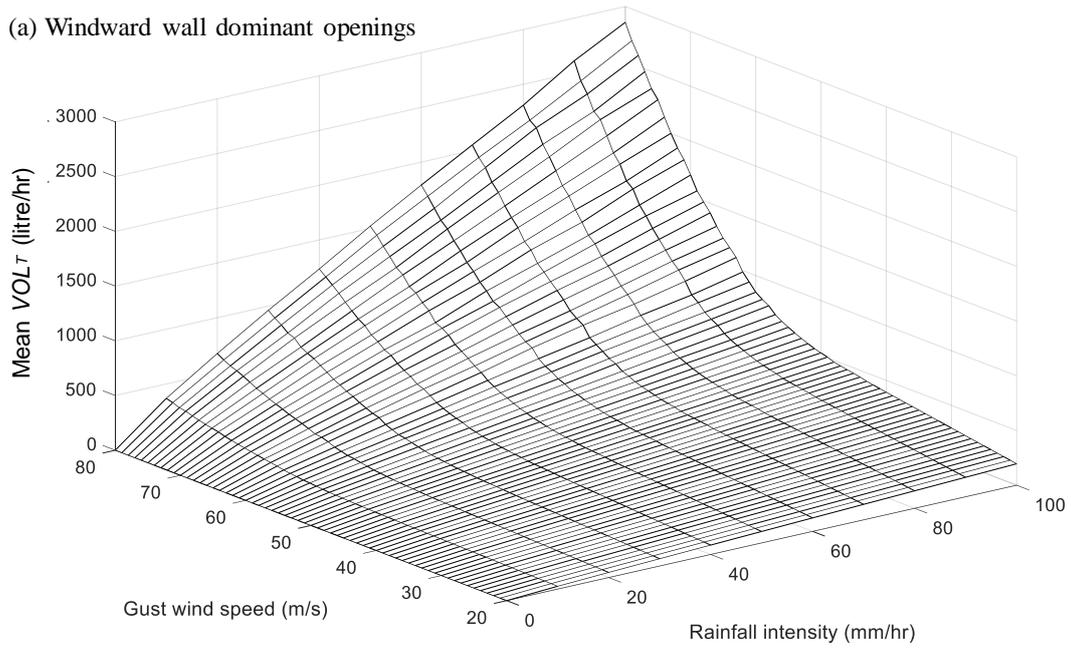
(b) No wall dominant openings
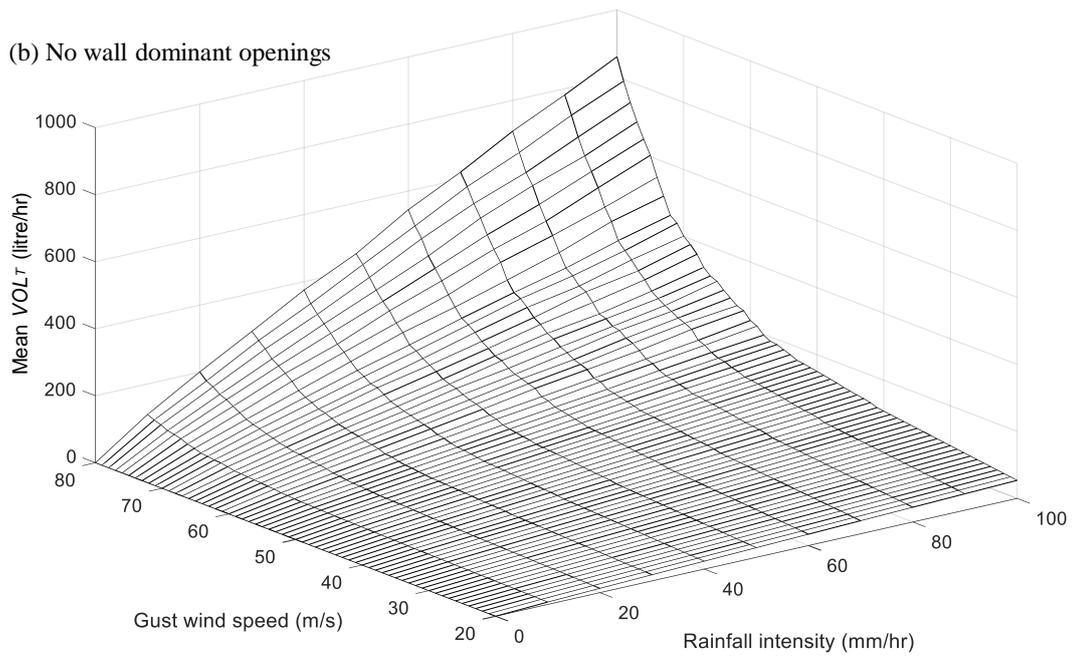
Figure 7. Mean VOL_T for two wall opening scenarios.
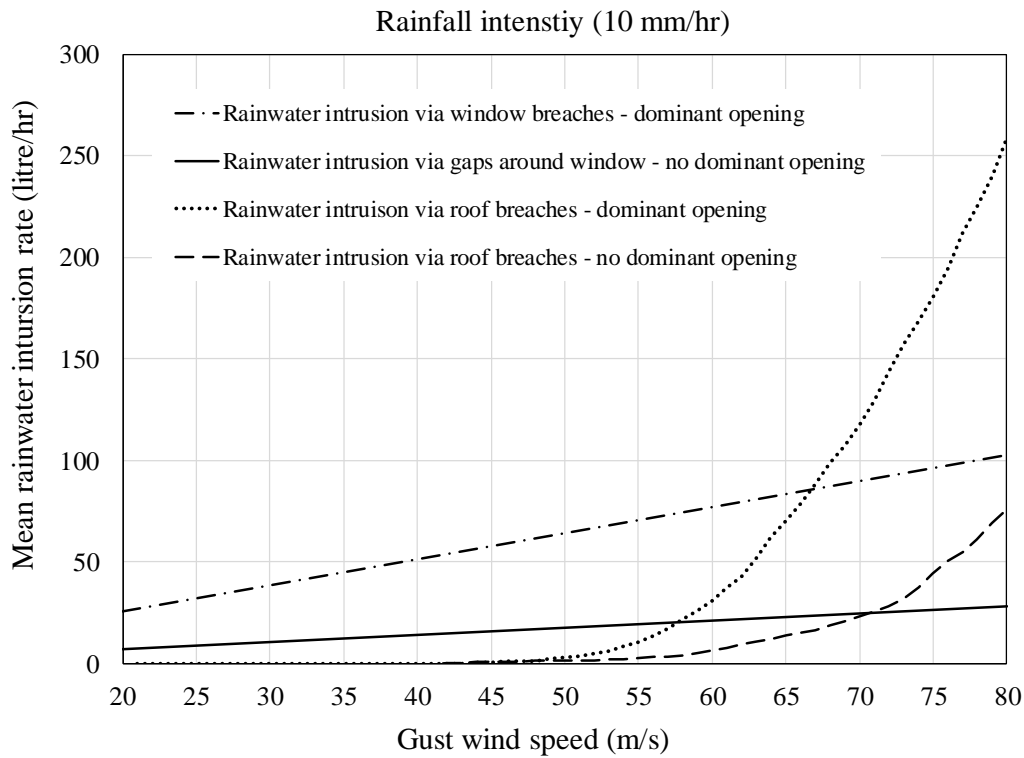
Figure 8. Mean volumetric rate of rainwater intrusion via roof and window respectively under the two wall opening scenarios at a rainfall intensity of 10 mm/hr.
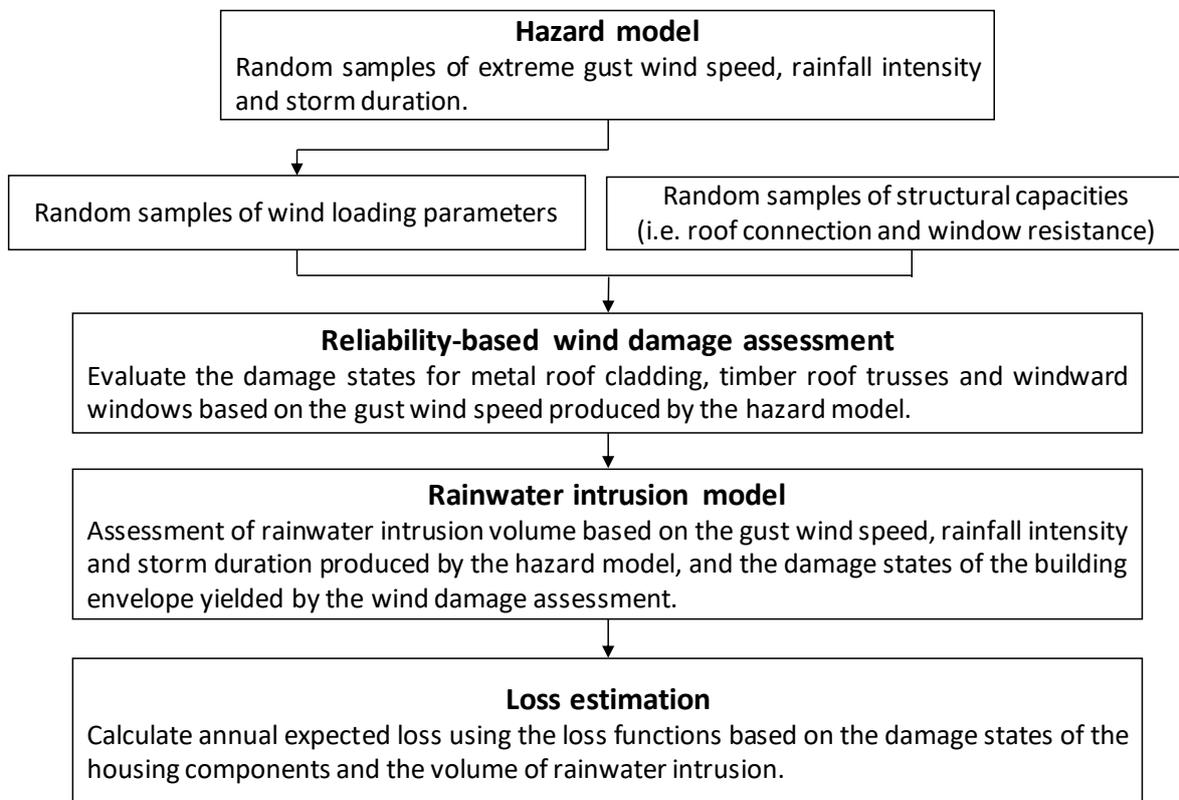
Figure 9. Outline of the risk analysis method.